



EFFECT OF VERTICAL BRACING ECCENTRICITY ON THE OUT-OF-PLANE BUCKLING OF STEEL COLUMNS

MOHAMED A. ABOKIFA¹, SHERIF M. IBRAHIM²,
ABDELRAHIM K. DESSOUKI³

¹Teaching Assistant, ²Associate Professor, ³Professor
Structural Engineering Department, Ain Shams University

المخلص

تتصل الشكالات في نظام الشكالات الرأسية بمنتصف عصب العمود في معظم الحالات و ذلك عندما يكون قطاع العمود على شكل حرف (I). ولكن في بعض الحالات نتيجة لظروف الإنشاء يتم تنفيذ هذه الوصلة بطريقة لا مركزية. تفحص هذه الدراسة السلوك و الإنخفاض في قدرة تحمل الأعمدة للإنبعاغ خارج المستوى نتيجة لامركزية وصلات الشكالات الرأسية. تم عمل دراسته واسعة النطاق عن طريق تحليل العناصر المحدده بطريقة غير خطية. تم فحص مختلف العوامل المؤثره مثل: التغير في قيم اللامركزية و تغيير قطاعات الأعمدة و اختلاف معاملات نحافة العمود للإنبعاغ خارج المستوى. تم عرض نتائج هذا البحث في صورة رسوم بيانية لإظهار تأثير كل عامل من هذه العوامل على إنخفاض قدرة تحمل العمود للحمل الرأسى نتيجة لوجود لامركزية في وصلات الشكالات الرأسية.

ABSTRACT

In most common situations, the strut member in the vertical bracing system is attached to the mid-point of web of the I-section columns. In certain situations due to constructional conditions, this connection is constructed eccentrically. This paper investigates the behavior and the reduction in the column out-of-plane buckling capacity due to the eccentricity in the vertical bracing connection. A non-linear finite element analysis is used to perform a wide range parametric study. Different parameters are examined such as: the variation of the eccentricity values, the different columns cross-sections and the various out-of-plane slenderness ratios. The results of this research are presented in graphs showing the influence of every parameter on the reduction in the axial column capacity due to the eccentricity in the vertical bracing connections.

Key words: Out-of-plane buckling, Finite element analysis, Eccentric bracing, Vertical bracing.

1. INTRODUCTION

I-section steel columns have mainly two failure modes. The first mode is in-plane buckling about the major axis, and the second mode is the out-of-plane buckling about the minor axis. The greater value of the two slenderness ratios ($\lambda=kl/r$) about the two axes will control the design. The out-of-plane buckling mode depends on the lateral bracing provided to the column in the longitudinal direction of the building. The strut members in the vertical bracing system are usually attached to the middle of the web of the I-section columns. The connection between those struts and the column web are constructed as simply supported joint, which provides lateral restraint to the column. In this ideal and most common situation the strut members can be represented as a pinned lateral support at the center line of the column. If the strut maintains the required ideal

stiffness to provide full lateral restraint to the column, the out-of-plane buckling factor will be equal to unity.

In certain situations because of some constructional conditions, the connection between the strut in the lateral bracing system and the web of the I-section column is constructed eccentrically. The current Egyptian code of practice for steel construction and bridges, (ECP No.250, 2008) and some other specifications such as AISC 2010 do not define a specific values for the out-of-plane buckling factors for such cases and most designers take this value by default as unity. The eccentricity of the connection of the strut member will affect the out-of-plane buckling mode and changes it from pure flexural buckling about minor axis to a combination of torsional and flexural buckling. In such cases, the equations provided in the Egyptian code of practice, (ECP No.250, 2008) and AISC 2010 will not be applicable.

Column bracing are classified into two main categories; lateral and torsional bracing. AISC 2010 specifications recommend that column bracing should resist lateral translation as well as twisting of the cross-section. In most practical situations, the lateral bracing does not have torsional stiffness. In this case, the torsional unbraced length may be greater than the flexural unbraced length, such that, the torsional strength of the column may govern the design. The ideal location for the lateral bracing is to be attached to the centroid of the cross section. Eccentricity in the location of the lateral bracing may lead to a reduction in the column axial capacity.

El-Banna et al. (2005) studied the effect of vertical bracing eccentricity on the out-of-plane buckling of H-shape steel columns. They used linear finite element analysis to perform a parametric study on seven sets of H-shaped columns from HEA 400 to HEA 1000. The parametric study results showed clearly that there was a reduction in the critical buckling load due to the eccentricity of the gusset plate connection and this reduction is directly proportional to the column depth. This reduction can reach 30% of the critical load compared to the case of no eccentricity.

Helwig and Yura (1999) studied the torsional buckling behavior of wide flange doubly symmetric columns with lateral bracing attached at different locations along the column cross-section. They used finite element analysis to determine the column's torsional capacity as well as the required torsional stiffness for the lateral bracing to make the torsional capacity (P_t) equal to the minor flexural capacity of column (P_y). The results of this study showed that; the torsional buckling capacity of columns with eccentric lateral bracing decreased as the distance between the bracing location and centroid "a" increased. It was required to provide a stiffer torsional brace in case the lateral bracing is attached eccentrically. In addition, the torsional bracing is not effective when the lateral bracing is attached away from the centroid of the cross-section.

The main aim of this research is to investigate the behavior of I-section steel columns with eccentric vertical bracing and their failure modes as well as to determine the reduction in the axial capacity for these columns. A verified non-linear finite element model is adopted to perform a wide range parametric study. This parametric study includes the effect of varying eccentricity ratios, using different columns cross-sections and varying column out-of-plane slenderness ratios.

2. FINITE ELEMENT MODEL

The main concept of the finite element method is that the complex engineering problems can be modeled easily using a finite number of elements whose displacement behavior is described by a number of displacement parameters known as the degrees of freedom. The objective of using finite element analysis in this study is to simulate the behavior of I-shaped steel columns in the out-of-plane buckling considering all material properties, dimensions of the studied members, boundary conditions and loading patterns. In this research, the analysis of the out-of-plane buckling of hot-rolled I-shaped columns is carried out by using ANSYS 14.5 finite element computer program. A detailed description of the developed finite element model is provided in the following sections.

2.1 DESCRIPTION OF THE PROPOSED MODEL

To study the out-of-plane buckling behavior of steel I-shaped columns, shell elements are used to simulate the components of the I-section columns as well as the used end plates in a three-dimensional model. In this research, four-node thin shell elements “SHELL 181” were used to model the investigated columns. “SHELL 181” is suitable for analyzing thin to moderately thick shell structures, it has both membrane and bending capabilities for the three dimensional analysis of structures. It is a four node element with six degrees of freedom at each node: translations in the x , y and z directions, and rotations about the x , y and z axes.

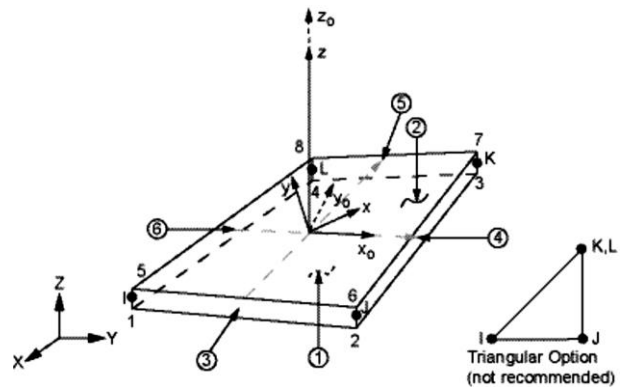


Figure (1): “SHELL 181” Geometry

“SHELL 181” is also suitable for linear analysis as well as large rotations and large strain non-linear applications and it also takes into account the change in shell thickness in non-linear analysis. Five integration points are designated along the thickness of each layer. The geometry, node locations and the coordinate system for this shell element are shown in Figure (1).

The mesh size used in the finite element model is adopted to provide accurate results and less analysis time as well as maintaining a reasonable aspect ratio. The thickness of the two attached end plates at both ends of the column is 30 mm. The purpose of using those plates is to ensure uniform distribution of the axial stress at the load application points and to overcome the problem of stress concentration at the location of the loading and supporting points.

To present the boundary conditions at column’s ends, a central node in the upper end plate is restrained from translation in two horizontal directions (U_x and U_z) in addition to rotation about the column longitudinal axis (R_y), while this end is free to move in the vertical direction in order to allow the axial deformation due to load application. On the other hand, a central node in the lower plate is restrained from translation in the three directions (U_x , U_y and U_z) in addition to rotation about the longitudinal axis (R_y). At the lower end plate all nodes on the line representing the web

of the column are restrained from translation in the vertical direction (U_y) in order to overcome the stress concentration in the column's web which may lead to local buckling failure. At mid-length of the column, a node is restrained from translation in the horizontal direction (U_x).

This point represents the vertical lateral bracing location. This location of the intermediate lateral bracing is varied along the web length to have eccentricity ratio (e/d) from "0.0" to "0.5" as shown in Figure (2).

The axial compressive force acting on the upper end of the analyzed column is represented as a group of equally concentrated loads distributed along the whole perimeter of the modeled column. These loads are raised incrementally through load steps until the column fails. The maximum capacity of the column is then calculated by multiplying the existing loads by the corresponding load factor. Figure (3) shows a typical schematic drawing for the column loading and restrained points.

Geometrical non-linearities are taken into account; with value of maximum imperfection taken as $1/1000$, where "1" is half column length.

Material non-linearities are taken into consideration by introducing a bilinear stress-strain curve with Young's modulus of elasticity ($E=2100 \text{ t/cm}^2$) and with tangent modulus ($E_t= 0.05 E$) to account for strain hardening. The yield strength (F_y) of the utilized steel is assumed to be equal to 2.4 t/cm^2 for Steel 37. The value of Poisson's ratio is taken equal to 0.3. The idealized stress-strain curve for Steel 37 is shown in Figure (4).

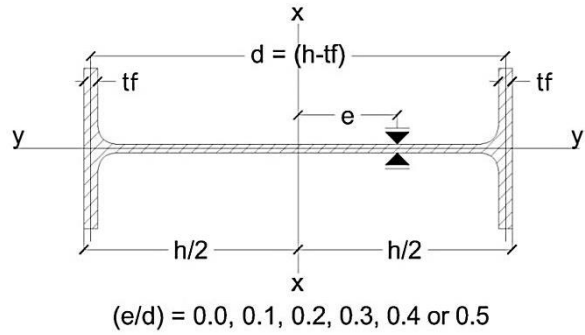


Figure (2): Eccentricity value (e/d)

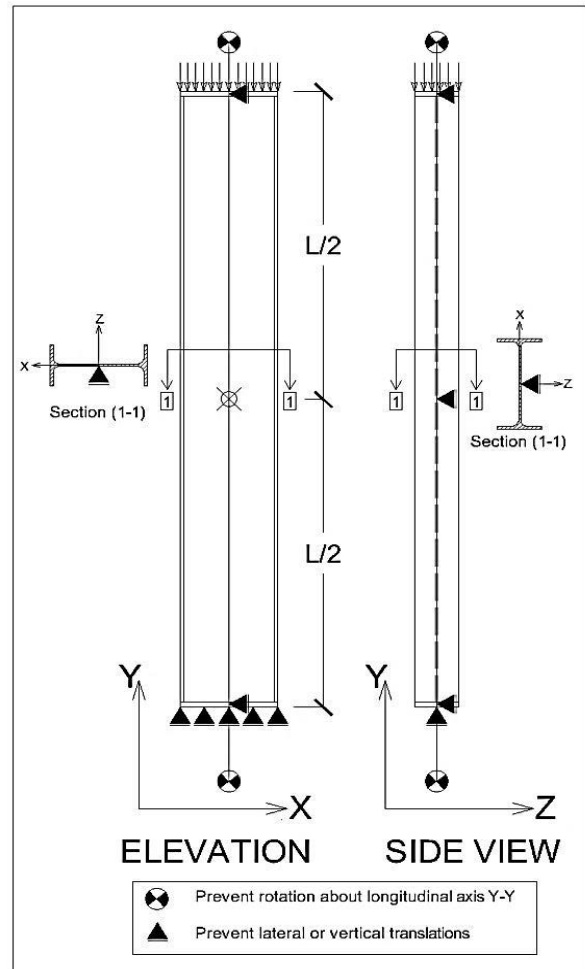


Figure (3): Typical schematic drawing for the column loading and restrained

The finite element analysis is conducted through two phases. The first phase is the linear buckling analysis, which is performed on a column having perfect geometry in order to obtain the probable elastic buckling modes of the modeled column. The second phase is the non-linear analysis of the buckled column obtained from the first

step. This phase is performed to obtain the ultimate capacity of the initially imperfect column as well as predicting the lateral deformations and failure mode of the examined column. Both material and geometrical non-linearities are incorporated in the non-linear static analysis which is performed by using the Modified Newton-Raphson (MNR) technique and employing the Arc-length control throughout the solution routine of the parametric study.

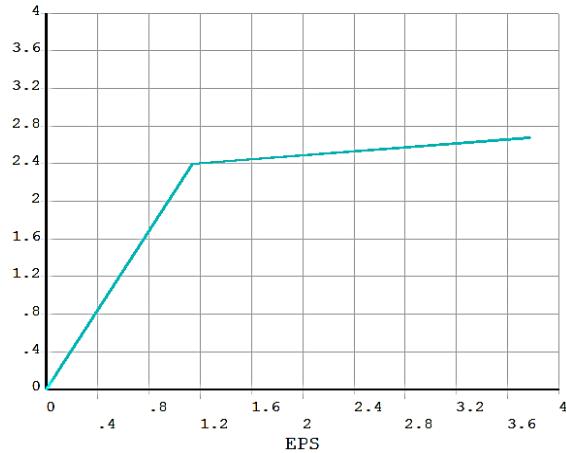


Figure (4): Idealized stress-strain curve for Steel 37

2.2 VERIFICATION OF THE PROPOSED MODEL

The main aim of this part is to verify the accuracy of results obtained from the finite element model. A set of comprehensive experimental works and published numerical results are selected to examine the accuracy of the finite element model. Verification study was performed under three different phases including verification with the nominal compressive strength equations provided in the AISC 2010 specifications, previous experimental work and previous results developed from nonlinear finite element analysis. Different cross-section geometries, material properties and loading conditions are examined in this study.

2.2.1 Verification with compressive strength equations in AISC 2010

The finite element analysis is carried out on two main phases. First, linear buckling analysis of the column was performed. Then, the linear buckling mode shape is scaled to define the imperfection for the non-linear analysis. The linear analysis results from the finite element model are verified with the theoretical results of the critical out-of-plane buckling load of a pin ended column determined using Euler formula as follows:

$$P_{cr} = P_E = \frac{\pi^2 E I_y}{l^2} \dots\dots\dots (1)$$

Where;

E: is the elastic modulus of steel,

I_y: is the moment of inertia of cross section about the y-axis, and

l: is the column buckling length in the out-of-plane direction.

On the other hand, the non-linear analysis results are compared with the nominal strength equations for the compression members specified in chapter “E” in AISC 2010 specifications.

A set of fifteen columns of type HEA 600 representing a wide range of slenderness ratios are examined, both the elastic and inelastic flexural buckling of columns about the minor axis are calculated. Finite element model is constructed to

determine the maximum compressive strength of the pin-ended columns supported laterally at its mid-length about the minor axis.

The comparison between results obtained from the linear and non-linear finite element analysis and those calculated from Euler formula and from the nominal strength equations for the compression members in the AISC 2010 specification are shown in Table (1). The finite element results give good correlation with the theoretical results and the results from AISC 2010 equations within a range of deviation +1.5 % and ± 5 % respectively.

specimen number	L/2 (cm)	kl/r _y	linear analysis			non-linear analysis		
			P _{FEM} (ton)	P _{EULER} (ton)	P _{FEM} /P _{EULER}	P _{FEM} (ton)	P _{AISC} (ton)	P _{FEM} /P _{AISC}
1	500	70.9	909.1	933.5	0.974	450.9	425.1	1.06
2	600	85.1	635.9	648.2	0.981	397.3	381.8	1.04
3	700	99.3	468.9	476.2	0.984	337.4	336.3	1.003
4	800	113.4	359.7	364.6	0.986	281.5	290.5	0.969
5	850	120.5	318.8	323.1	0.987	256.5	268.1	0.957
6	900	127.6	284.5	288.1	0.987	234.1	246.2	0.951
7	950	134.7	255.5	258.5	0.988	214.1	224.9	0.951
8	985	139.7	237.7	240.5	0.988	201.3	210.4	0.956
9	1000	141.8	230.6	233.3	0.988	196.2	204.1	0.961
10	1050	148.9	209.2	211.6	0.988	180.2	185.1	0.973
11	1100	156.1	190.7	192.8	0.988	166.1	168.7	0.974
12	1150	163.1	174.5	176.4	0.989	153.3	154.3	0.993
13	1200	170.2	160.3	162.0	0.989	142.0	141.7	1.001
14	1300	184.4	136.6	138.1	0.989	122.6	120.8	1.015
15	1410	200	116.1	117.4	0.989	105.5	102.6	1.027

Table (1): Comparison of finite element and nominal strength equations for the compression members in the AISC 2010 specification

2.2.2 Verification with previous experimental and numerical researches

This section contains verification with three different experimental studies as well as one numerical research. A total of nine different specimens from previous experimental studies and nine different specimens from previous numerical research were used in the verification.

(1) The first experimental research was carried out by (Wang et al. 2014), who studied strengthened steel columns to investigate the effect of initial load on mechanical properties of steel columns after weld strengthening processes. The load-carrying

behavior of I-section steel columns strengthened by welding with initial load is examined. The control specimen from their work was chosen in the current verification study. The tested member is a long column that failed by flexure buckling about its minor axis. The end constraint of the steel column used single hinged support to maintain the rotation around the weak axis. Rigid end plates were connected to the test specimen at both ends during testing. All the required data about the specimen were reported such as column's full dimensions, the material properties, the yield stress and the modulus of elasticity were measured using tensile coupons. Three measures were done of the initial imperfections along the column length as well as the measures of the eccentric value of the applied axial load. Figure (5) shows the specimen dimensions and its out-of-straightness values.

$L=2999.5 \text{ mm}, H= 257.5 \text{ mm}, t_w=9.87 \text{ mm}, b_f=179.3 \text{ mm}$ and, $t_f=7.87 \text{ mm}$
 $\delta_1= -0.047 \text{ mm}, \delta_2= -0.223 \text{ mm},$ and $\delta_3= -0.375 \text{ mm}$

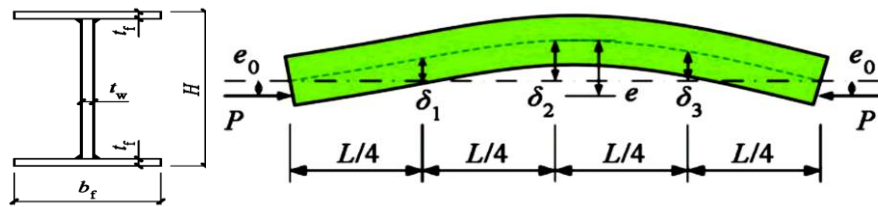


Figure (5): Cross section dimensions and out-of-straightness values of the control specimen (Wang et al. 2014)

Comparison between results of the experimental study performed by (Wang et al. 2014) and the results obtained from the non-linear finite element analysis is shown in Table (2). It is obvious that the finite element result is in good agreement with the experimental result with deviation equal to 3.6 %.

$P_{\text{EXPERIMENT}}$ (ton)	P_{FEM} (ton)	$P_{\text{FEM}} / P_{\text{EXP}}$
111.525	107.548	0.964

Table (2): Comparison of finite element and experimental results of control test specimen column tested by (Wang et al. 2014)

(2) The second experimental research was performed by Bjorhorde (1972), who utilized the deterministic and probabilistic approaches to investigate the strength of centrally loaded, pinned-end, initially curved, prismatic steel columns. Two steel rolled wide-flange columns were chosen to be verified from a large set of tested columns including rolled and welded wide-flange columns and welded box columns. Both of the tested specimens failed by flexure about their minor axes. All the required data about both specimens were indicated such as columns cross-section, material properties, residual stresses and initial imperfections.

Comparison between results of the experimental study performed by (Bjorhovde, 1972) and the results obtained from the non-linear finite element analysis are shown in Table (3). It is obvious that the finite element results are in good agreement with the experimental results with maximum deviation equal to 8.7 %.

(3) The third experimental research was carried out by (Feng et al. 2013), who performed experimental and numerical investigations on high strength steel welded H-section columns. A series of six tests was carried out on different geometries of welded H-section columns fabricated from high strength steel with nominal yield stress of 460 Mpa.

specimen number	column section	steel grade	Experiment				F.E.M	P_{FEM} / P_{EXP}
			e/L	λ	l/r	P_{EXP} / P_y	P_{FEM} / P_y	
1	W8x31	A242	0.0009	0.75	54	0.82	0.89	1.087
2	W12x120	A514	0.0002	0.92	50	0.82	0.88	1.073

Table (3): Comparison of finite element and experimental results of I-section columns tested by (Bjorhovde, 1972)

Beside their experimental study, Feng et al. (2013) conducted finite element analysis on high strength steel welded H-section columns. The finite element modeling was conducted for the tested specimens as well as performing a limited parametric study on different columns cross-sections. A set of nine columns were modeled and examined. The non-linear finite element program used in that study was ABAQUS 6.10. Both linear perturbation analysis and non-linear analysis were performed to obtain the ultimate strengths and failure modes of the high strength steel columns. Both material and geometrical nonlinearities were taken into consideration. However, modeling of residual stresses was not taken into account. Their finite element mesh was varied to provide accurate results as well as less analysis time. Their finite element model takes into consideration all the measured data of the tested specimens such as the measured dimensions and the material properties. The load transfer plates at specimen's ends were modeled using analytical rigid plates. The same end conditions used in the numerical study of the specimens were accurately considered in the modeling.

Comparison between results of the experimental and numerical study performed by (Feng et al. 2013) and the results obtained from the current non-linear finite element analysis are shown in Table (4) in addition to the dimensions of the investigated specimens. It is obvious that the finite element results are in good agreement with the experimental results as well as the numerical results within an average range of deviation 11.2 % for the former and ± 1 % for the later.

specimen number	length (mm)	specimen dimensions (mm)			Experiment	F.E.M	Current F.E.M	$P_{FEM(2)} / P_{FEM(1)}$	$P_{FEM(2)} / P_{EXP}$
		h_w	b_f	t_w or t_f	Feng et al. 2013	Feng et al. 2013	Feng et al. 2013		
					P_{EXP} (ton)	$P_{FEM(1)}$ (ton)	$P_{FEM(2)}$ (ton)		
L1	2120	203.6	151.6	10.82	162.25	186.49	188.00	1.008	1.158
L2	2719	201.5	151.8	10.39	114.15	129.72	128.53	0.991	1.126
L3	3318	199.1	151.8	11.08	83.95	99.94	98.99	0.991	1.179
L4	2120	201.2	149.9	12.74	212.8	204.62	205.69	1.005	0.966
L5	2720	200.3	150.8	12.47	129.8	147.50	144.93	0.983	1.116
L6	3321	202.2	151.6	12.65	114.3	112.058	107.84	0.962	0.943
L7	1060	190	150	10	NA	253.48	249.40	0.984	NA
L8	1660	190	150	10	NA	191.28	194.70	1.018	NA
L9	2860	190	150	10	NA	99.93	102.04	1.021	NA

Table (4): Comparison of finite element with experimental finite element results of high strength steel I-section columns tested by (Feng et al. 2013)

In conclusion, the results obtained from the finite element model were found to be in very good agreement with the results obtained from the equations of AISC 2010 specifications as well as the previous experimental and numerical studies.

3. PARAMETRIC STUDY

A parametric study is performed to determine the out-of-plane buckling capacity of I-section steel columns using eccentric vertical bracing with respect to their webs. The parametric study can be classified into two main sections in which different parameters are introduced and investigated. A total number of 468 specimens were studied. The main parameters investigated in this study are discussed in the following sections:

i. Effect of eccentricity ratio (e/d):

The eccentricity ratio in this part of study varied from “zero” to “0.5” with increment “0.1”. The study is performed on seven cross-sections namely; IPE600, IPE400, IPE 300, HEB 1000, HEB 800, HEB 700 and HEB 500. All specimens have pin-ended boundary conditions and lateral bracing is located at mid-length (i.e. $a/L=0.5$). Various out-of-plane slenderness ratios (Kl/ry) of 60, 70, 80, 100, 120, 140, 160, 180 and 200 were considered. The material considered in this study is Steel 37 with yield strength 240 N/mm^2 .

ii. Effect of steel cross-section type:

Three steel profiles namely HEA 1000, HEB 1000 and HEM 1000 are considered in this part. The three cross-sections are investigated for eccentricity ratios

$e/d = 0.0, 0.1, 0.2, 0.3, 0.4$ and 0.5 . The out-of-plane slenderness ratio (Kl/r_y) is taken equal to “80” and material considered is Steel 37.

To broaden the study of the effect of steel cross-section type, complete sets of IPE, HEA, HEB and HEM sections are investigated. This part of the study is carried out for eccentricity ratios (e/d) “0.0” and “0.5” only with lateral bracing at mid-length (i.e. $a/L = 0.5$) and out-of-plane slenderness ratio (Kl/r_y) equals “80”.

4. DISCUSSION OF RESULTS

The results of the parametric study are shown in the form of graphical relationships. Three main types of graph sets are used in this section. The first set represents the relation between “ P_{FEM}/P_y ” and the out-of-plane slenderness parameter “ Kl/r_y ”. The second graph set represents the relation between “ $P_{e/d=0.5}/P_{e/d=0.0}$ ” and column cross-section depth “ d ”. The third graph set represents the relation between “ P_{FEM}/P_y ” and the eccentricity ratio “ e/d ”. These parameters are defined as follows:

P_{FEM} : maximum nominal strength of the investigated columns obtained from non-linear finite element analysis.

- P_y : yield strength of the column. Where: $P_y = A_{total} \times F_y$ (2)
 A_{total} : is the total area of the column cross-section,
 F_y : is the yield stress of the used steel.
- Kl/r_y : is the out-of-plane slenderness parameter of the column.
 K : is the effective length factor and its value is usually taken equal to unity,
 l : is half the column length,
 r_y : is the column cross-section minor radius of gyration.
- $P_{e/d=0.5}$: is the maximum nominal strength obtained from non-linear finite element analysis of the column which has eccentric vertical bracing attached to their flange.
- $P_{e/d=0.0}$: is the maximum nominal strength obtained from non-linear finite element analysis of the column which has centric vertical bracing attached at the middle of its web.

The results of the parametric study can be summarized as follows:

4.1 Effect of eccentricity ratio (e/d):

Error! Reference source not found., (7) and (8) show the relationship between “ P_{FEM}/P_y ” and “ Kl/r_y ” for IPE 600, IPE 400 and IPE 300 columns respectively. The most common trend detected in those graphs is that the ultimate axial capacity of the columns decreases with the increase of the eccentricity value (e/d). This happens due to the difference between the developed buckling shapes of the columns which have concentric vertical bracing to their webs and those having eccentric vertical bracing. Figure (9) and (10) show the two different buckling shapes respectively.

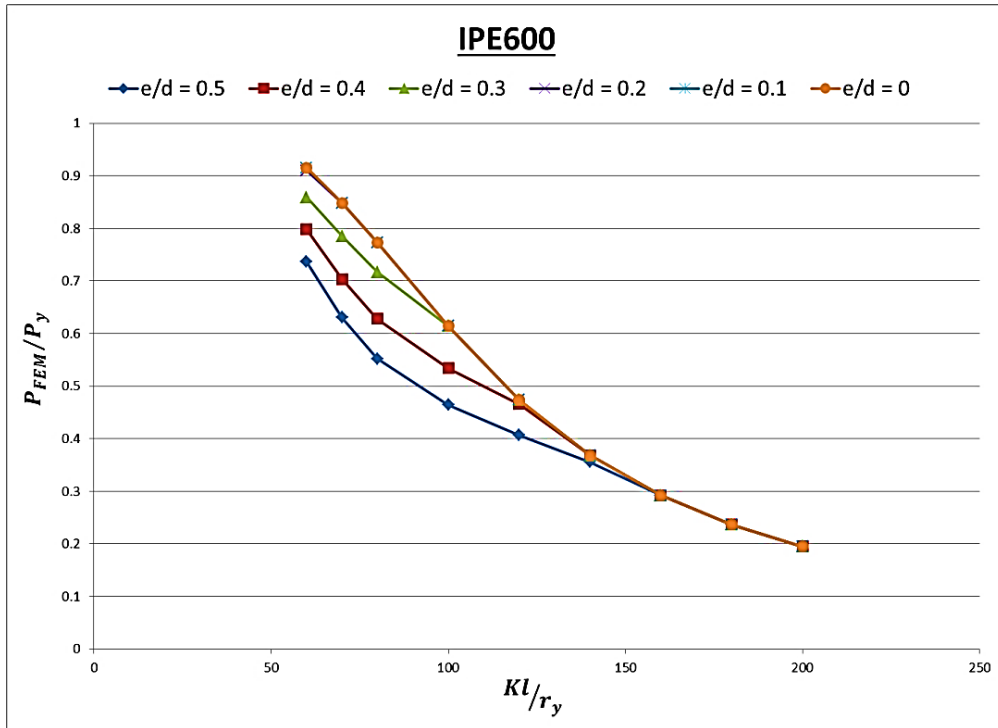


Figure (6): P_{FEM}/P_y versus $K1/r_y$ for IPE 600 column supported at mid-length for different e/d ratios

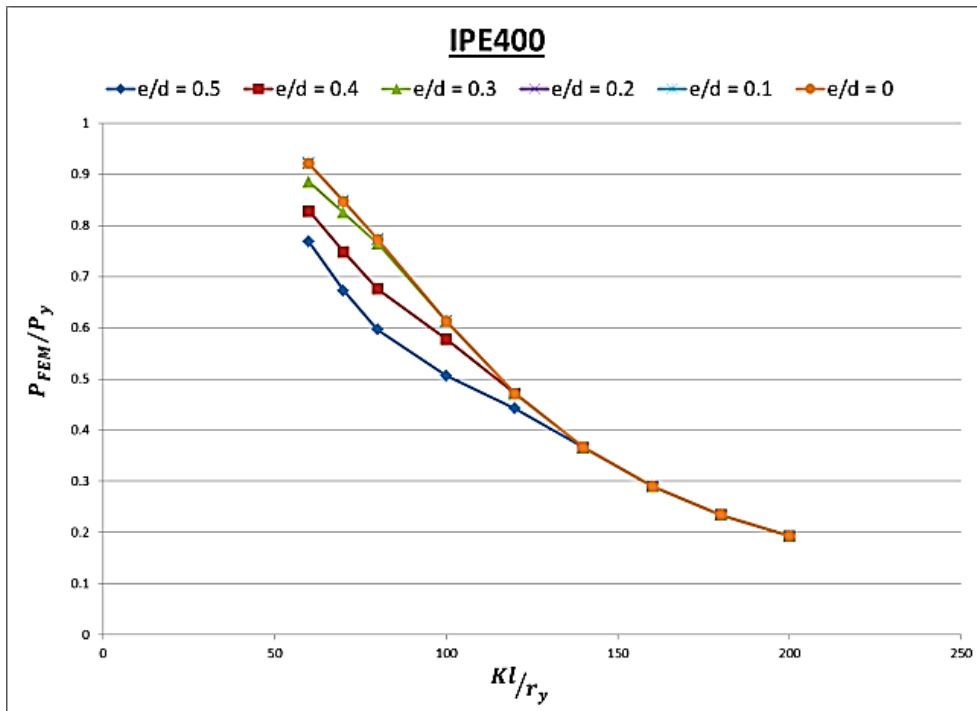


Figure (7): P_{FEM}/P_y versus $K1/r_y$ for IPE 400 column supported at mid-length for different e/d ratios

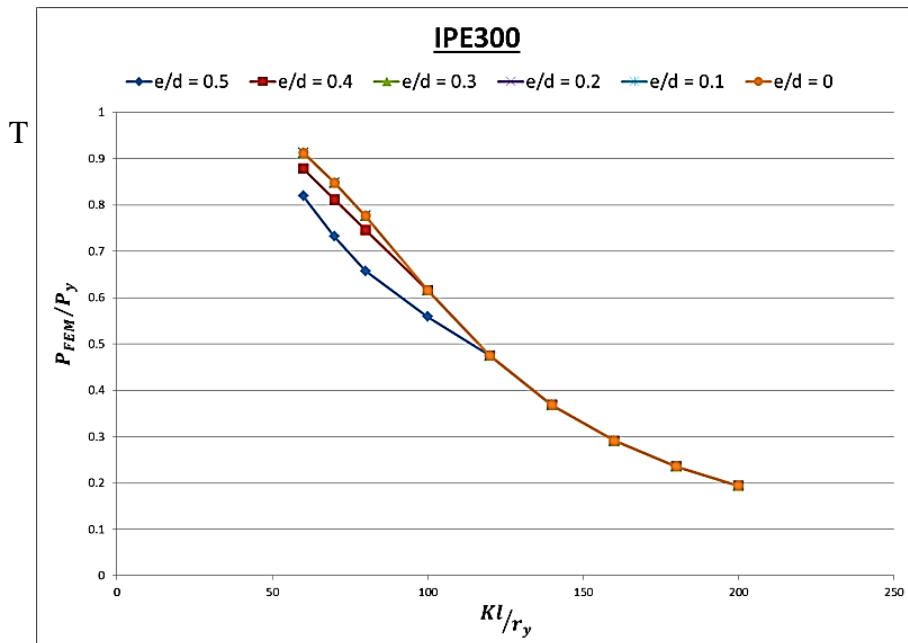


Figure (8): P_{FEM}/P_y versus K_l/r_y for IPE 300 column supported at mid-length for different e/d ratios

The first buckling mode shape in Figure (9) represents the ideal case for a pinned-end column which is laterally supported at its mid-length and its mid-web. For this case the column undergoes pure global buckling about its minor axis. The ultimate capacity of this column can be well predicted by the nominal strength equations for the compression members specified in chapter “E” in AISC 2010 specifications.

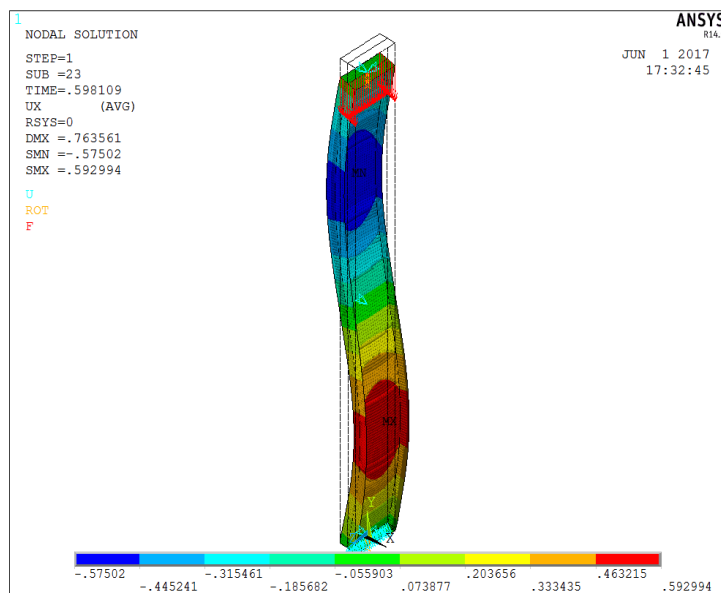


Figure (9): Buckling shape of IPE 600 column with $(K_l/r_y=80)$ and supported at mid-length with concentric vertical bracing

The second buckling mode shape in Figure (10) represents the case in which the column has eccentric vertical bracing to its web with eccentricity ratio ($e/d = 0.5$). It is clear that the buckling shape has changed from the first case and it tends to be a combination between lateral and torsional buckling along the total length of the column. Consequently, the column with eccentric bracing, cross-section will rotate around the laterally supported points to develop a buckling shape similar to that of the singly symmetric columns. The vertical bracing joint prevents lateral translation only while the torsional buckling of the column may govern its axial capacity and would be smaller than flexural buckling about its minor axis.

The effect of using eccentric vertical bracing to column web is significant for short columns or in another words; columns with small out-of-plane slenderness values (Kl/r_y). On the other hand, this effect is not recognized for long “elastic” columns. This is because the torsional buckling is dominant for short columns while flexural buckling about minor axis is dominant for long columns.

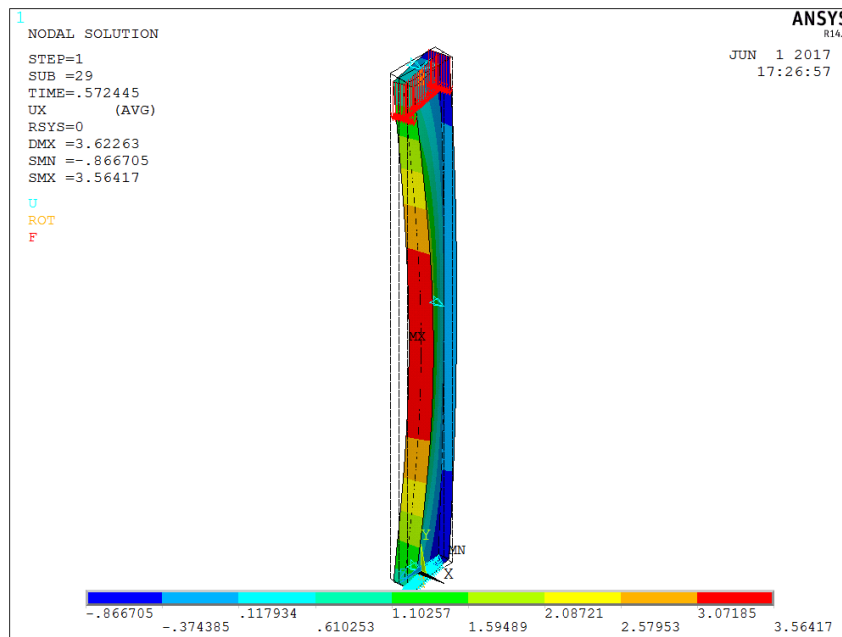


Figure (10): Buckling shape of IPE 600 column with ($Kl/r_y=80$) and supported at mid-length with eccentric vertical bracing with eccentricity ratio ($e/d=0.5$)

It is clear that the small eccentricity ratio values such as ($e/d=0.1, 0.2$), the ultimate axial capacity of columns is not affected by such eccentricity ratio values. This is observed for IPE 600 and IPE 400 columns, while for IPE 300 the eccentricity ratios ($e/d=0.1, 0.2$ and 0.3) will not affect the column axial capacity. The main reason for this is that for small eccentricity ratios (e/d) the column undergoes flexural buckling about its minor axis as the vertical bracing will prevent lateral translation as well as twisting of the column cross-section.

Figure (11) shows the relationship between “ P_{FEM}/P_y ” and eccentricity values “ e/d ” for IPE 600, IPE 400 and IPE 300 columns with out-of-plane slenderness ratio ($Kl/r_y=80$).

It is observed that the maximum drop in the axial capacity of columns with eccentric vertical bracing with respect to capacity of columns with concentric vertical bracing occurs for columns with out-of-plane slenderness ratio (Kl/r_y) equal to 80. The maximum drop in axial capacity of IPE 600, IPE 400 and IPE 300 columns with eccentricity ratio ($e/d=0.5$) is 29%, 23% and 16% respectively.

As the depth of column cross-section increases, the drop in column capacity with eccentric vertical bracing increases. For IPE 600 column the maximum drop in capacity is 29%. Columns with out-of-plane slenderness ratios (Kl/r_y) smaller than 160 are affected by the eccentricity of vertical bracing. On the other hand, the maximum drop in capacity for IPE 300 is 16%. Columns with out-of-plane slenderness ratios (Kl/r_y) smaller than 120 are affected by the eccentricity.

For a given (e/d) ratio, as the depth of column increases, the eccentricity parameter (e) of bracing will increase and this will lead to larger drop in the axial capacity. That is why larger column depth is usually accompanied with larger drop in the axial capacity.

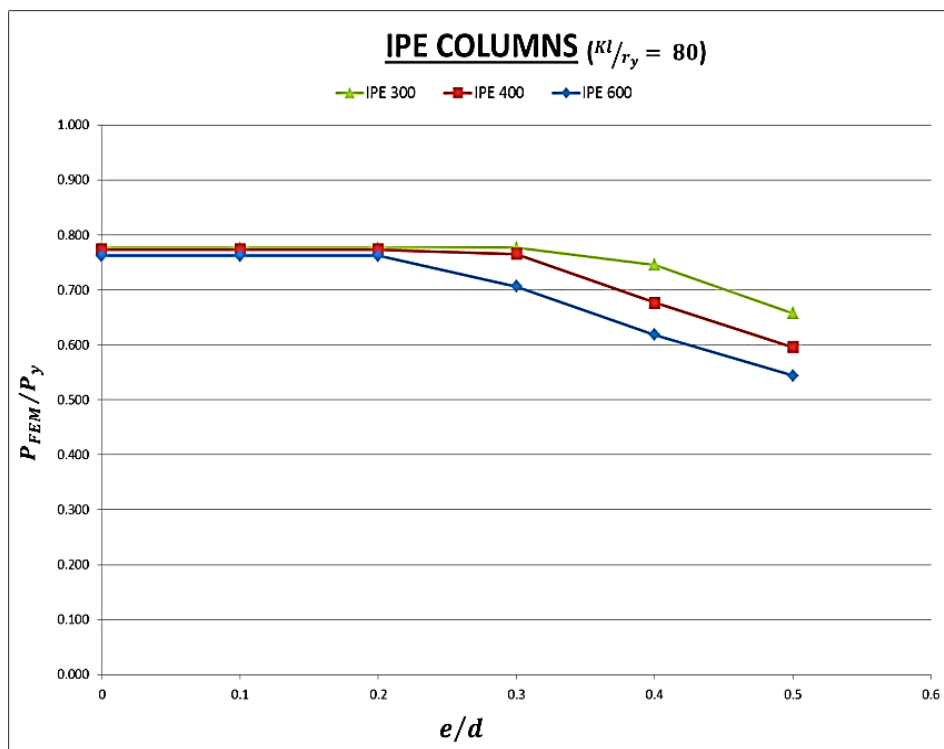


Figure (11): P_{FEM}/P_y versus e/d for set of IPE columns with ($Kl/r_y=80$) and supported at mid-length

4.2 Effect of using different cross-section types:

Figures (12), (13), (14) and (15) show the relationship between “ P_{FEM}/P_y ” and “ Kl/r_y ” for HEB 1000, HEB 800, HEB 700 and HEB 500 columns respectively. It is clear that despite using different types of cross-sections which have high rigidity against twisting and flexural buckling about minor axis. The same results observed for IPE sections are also observed here but with some little changes.

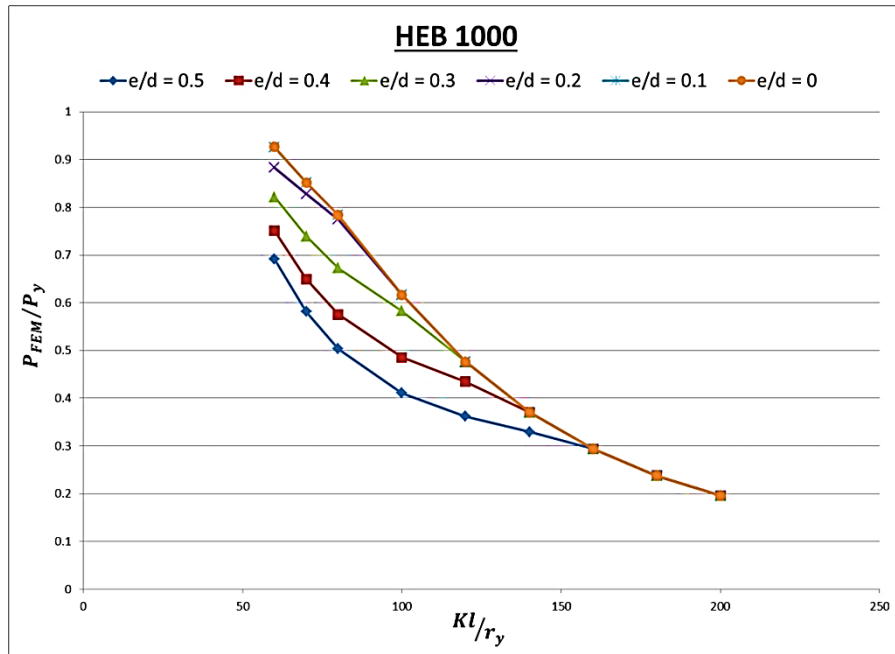


Figure (12): P_{FEM}/P_y versus Kl/r_y for HEB 1000 column supported at mid-length for different e/d ratios

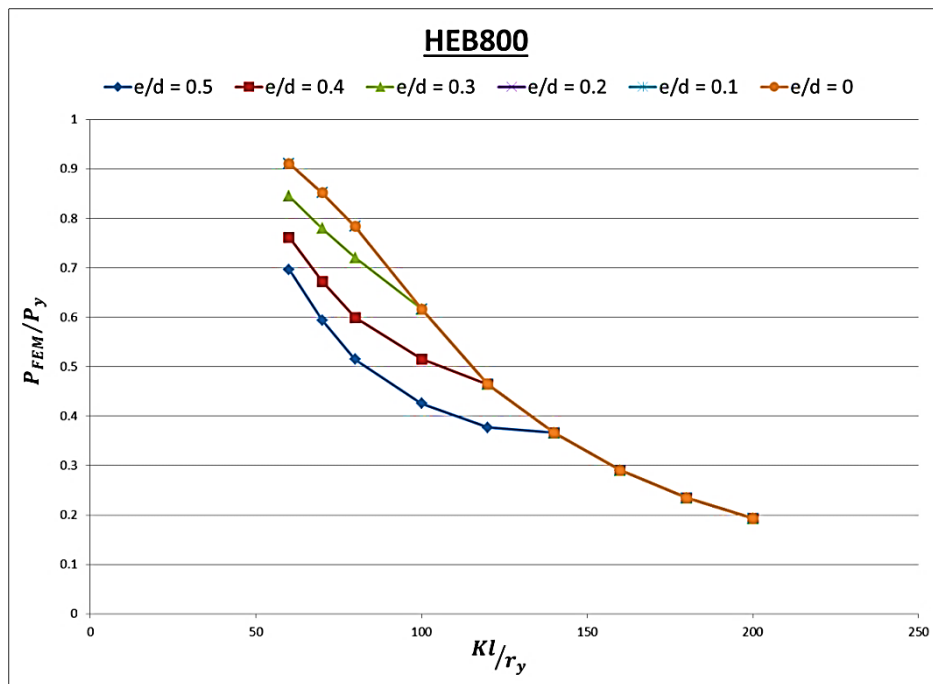


Figure (13): P_{FEM}/P_y versus Kl/r_y for HEB 800 column supported at mid-length for different e/d ratios

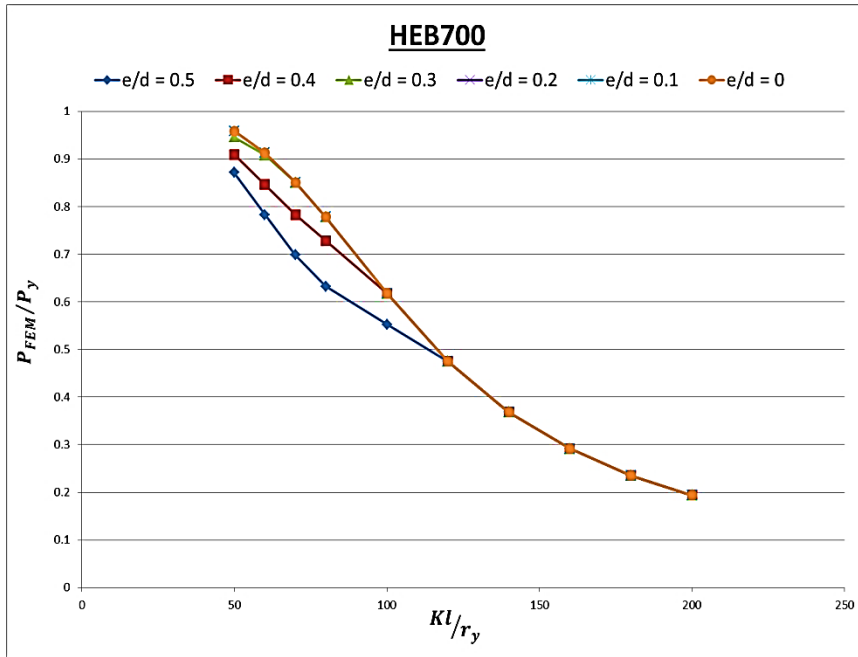


Figure (14): P_{FEM}/P_y versus Kl/r_y for HEB 700 column supported at mid-length for different e/d ratios

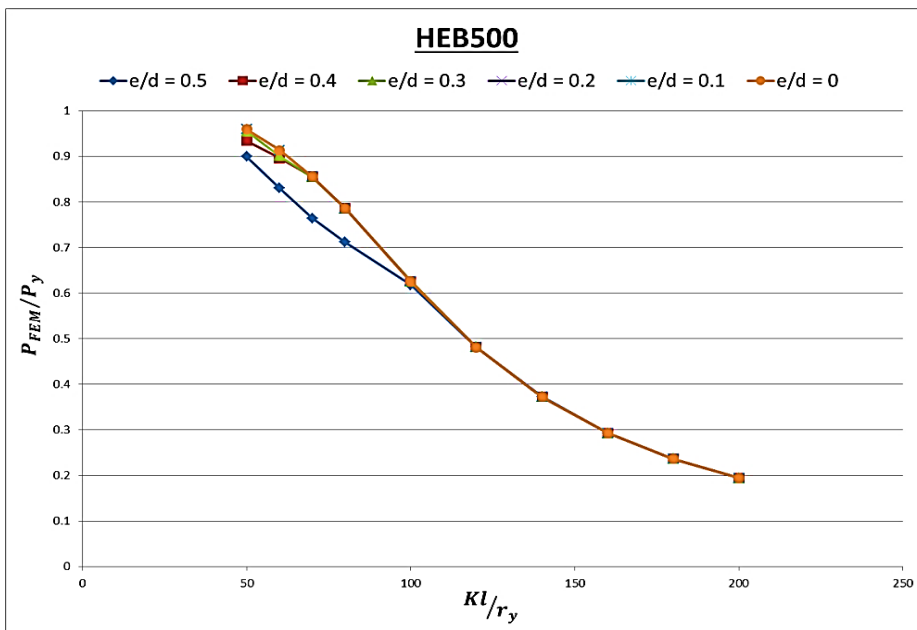


Figure (15): P_{FEM}/P_y versus Kl/r_y for HEB 500 column supported at mid-length for different e/d ratios

A comparison between HEB 500 and IPE 400 columns is done in order to verify the difference in behavior resulting from changing the type of column cross-section. The maximum drop in the axial capacity of HEB 500 column with eccentricity ratio ($e/d=0.5$) is only 11% while this drop for IPE 400 is 23% which is bigger than the drop of HEB 500 although IPE 400 section has a smaller depth than HEB 500. This main

difference between these types of sections can be attributed to the ability of HEB section to resist twisting as well as out-of-plane flexural buckling. The HEB 500 column which has a bigger rigidity for twisting is not greatly affected by using eccentric vertical bracing so that the only eccentricity ratio (e/d) which has an effect on the axial capacity of this column is the extreme case in which eccentricity ratio ($e/d=0.5$). For IPE 400 column, eccentricity ratios ($e/d=0.3, 0.4$ and 0.5) have an effect on the axial capacity of the column.

The benefit of using a type of cross-section which has high rigidity for twisting with columns that have eccentric vertical bracing is vanished gradually when using bigger column depths. As clear for HEB 1000 the maximum drop in the axial capacity of the column with eccentricity ratio ($e/d=0.5$) compared to that with concentric bracing is approximately 40% and the out-of-plane slenderness ratios (Kl/r_y) smaller than 160 are affected by eccentric bracing with eccentricity ratios ($e/d=0.2, 0.3, 0.4$ and 0.5). Therefore, the fact that using a type of cross-section with high torsional rigidity will limit the drop in axial capacity with eccentric vertical bracing is only applicable for columns with smaller cross-section depths.

Figure (16) shows the relationship between “ P_{FEM}/P_y ” and eccentricity values “ e/d ” for HEB 1000, HEB 800, HEB 700, HEB 500 and HEB 200 columns with out-of-plane slenderness ratio ($Kl/r_y=80$). It is evident from this graph that the effect of using eccentric vertical bracing is significant with columns which have a bigger cross-section than HEB 500, while this observation is not recognized with IPE columns. IPE columns with smaller depths are affected by the eccentricity in vertical bracing.

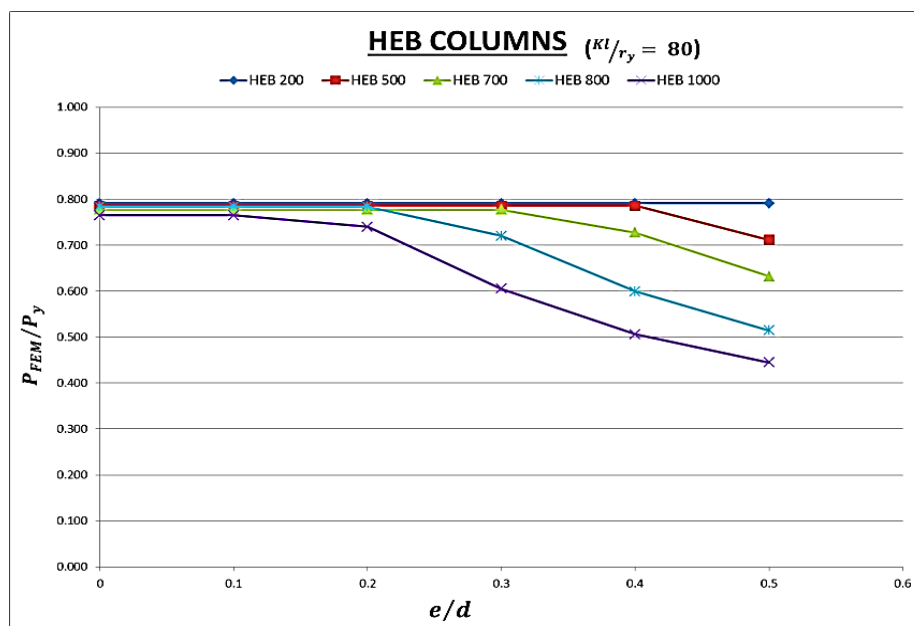


Figure (16): P_{FEM}/P_y versus e/d for set of HEB columns with $(Kl/r_y=80)$ and supported at mid-length

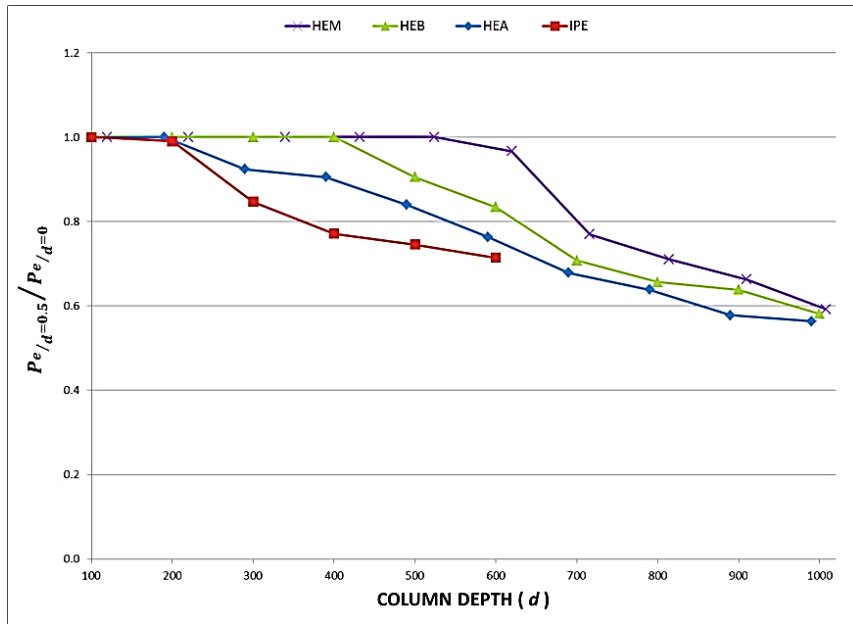


Figure (17): P_{FEM}/P_y versus e/d for set of HEB columns with $(K_1/r_y=80)$ and supported at mid-length

To know the range of hot rolled columns which has significant drop in the axial capacity when using eccentric vertical bracing, another study is performed on a number of different types of hot rolled columns with out-of-plane slenderness ratio $(K_1/r_y = 80)$ and eccentricity ratios (e/d) equal to 0.0 and 0.5. Steel 37 is used in this study. The results of this study are represented in Figure (17). It is clear that the axial capacity of the columns with eccentric vertical bracing decreases with the increase of the depth of the column cross-section. For any column depth, the drop in the axial capacity for columns with high torsional rigidity is smaller than that of columns with small torsional rigidity.

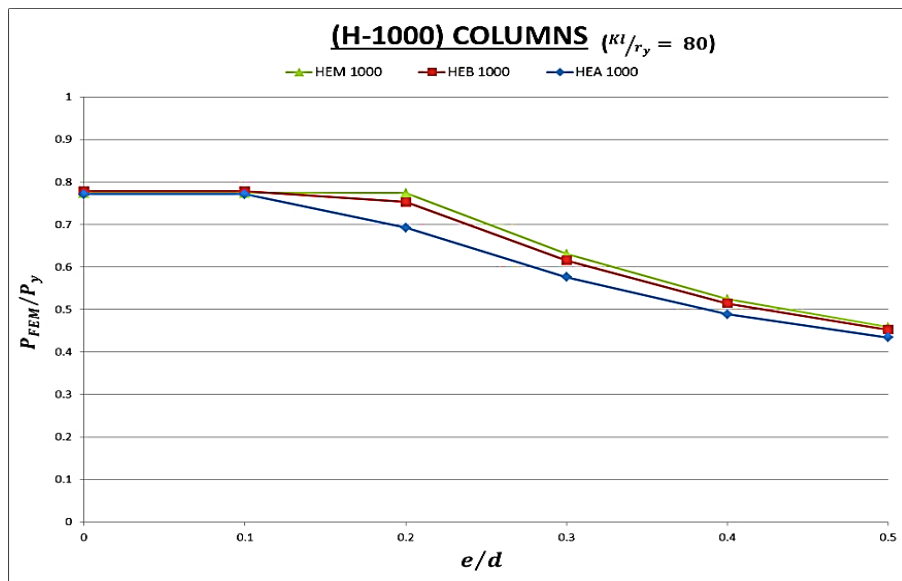


Figure (18): P_{FEM}/P_y versus e/d for set of (H-1000) columns with $(K_1/r_y=80)$ and supported at mid-length

To investigate thoroughly the effect of using different cross-section types on the drop of capacity of columns without the contribution of column cross-section depth, a study is conducted on HEA 1000, HEB 1000 and HEM 1000 columns which approximately have equal depths and with out-of-plane slenderness ratio ($Kl/r_y=80$). The results of this study are represented in Figure (18). It is evident that as the column torsional rigidity increases, the drop in capacity developed from using eccentric vertical bracing decreases. The torsional rigidity of a certain column is dependable on the torsional constant of the section (J). For HEM 1000 column the value of “ J ” is bigger than that of HEA 1000, thus the drop in capacity for HEM 1000 is smaller than of HEA 1000.

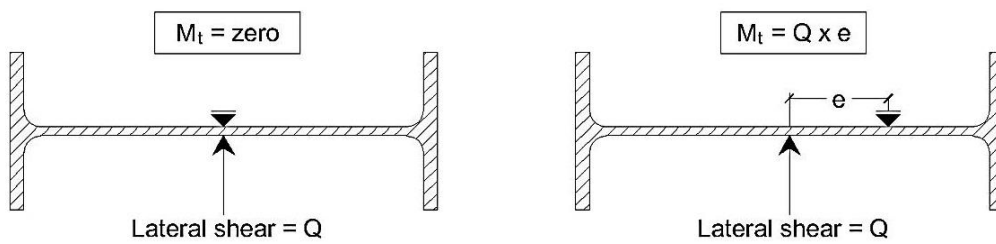


Figure (19): Developed torsional moment

The buckling mode developed from using eccentric vertical bracing to column web is torsional buckling as shown in Figure (10). This buckling mode refers to the presence of torsional moment applied to the column cross-section. This torsional moment can be explained as a result from the action of lateral shear acting about the center of rotation (i.e. the eccentric bracing location) as shown in Figure (19).

For doubly symmetric I-section columns the shear center will coincide with the center of gravity. But in case of using eccentric vertical bracing, the column will twist around the supporting point. Therefore, the developed torsional moment depends on the eccentricity parameter (e) which represents the distance between the center of gravity and the point where the column cross-section undergoes torsion. The eccentricity parameter (e) is a factor of the column depth. The investigated eccentricity ratio ($e/d=0.5$) means that the eccentricity parameter (e) will be equal to half the column depth. Thus for columns with large depth cross-sections, the eccentricity parameter (e) will increase which will lead to an increase in the torsional moment.

5. CONCLUSIONS

- 1- The ultimate axial capacity of columns decreases with the increase of the eccentricity ratio (e/d).
- 2- The effect of using eccentric vertical bracing to column web is significant for short columns, while this effect is not significant for long “elastic” columns.
- 3- Small eccentricity values do not affect the axial capacity of columns, while, large eccentricity values reduce the column axial capacity as the governing mode of buckling will be torsional buckling.

4- The maximum drop in the axial capacity of columns with eccentric vertical bracing is specified for columns with out-of-plane slenderness ratio (Kl/r_y) equal to 80.

5- As the depth of column cross-section increases, the drop in capacity developed from using eccentric vertical bracing increases and the range of columns influenced by this eccentricity increases while the opposite is true.

6- For certain column depth, the drop in the axial capacity for columns with high torsional rigidity is smaller than that of columns with small torsional rigidity.

7- Using cross-sections having high torsional rigidity in case of eccentric vertical bracing is only effective in increasing column capacity for columns with smaller cross-section depths.

6. REFERENCES

[1] Mahmoud El-Banna, Sherif M. Ibrahim, Ahmed H. Yousef (2005) "Effect of Vertical Bracing Eccentricity on The Out-of-Plane Buckling of H-Shape Steel Columns", Eleventh International Conference on Structural and Geotechnical Engineering.

[2] AISC Specifications for structural steel buildings, Load and Resistance Factors Design (LRFD) (2010)

[3] Joseph A. Yura (2001) "Fundamentals of Beam Bracing" Engineering Journal, First Quarter.

[4] Plaut, R. S. (1993), "Requirements for Lateral Bracing of Columns with Two Spans," Journal of Structural Engineering, ASCE, Vol. 119, No. 10, October, pp. 2913-2931.

[5] Timoshenko, S. and Gere, J., (1961), Theory of Elastic Stability, New York: McGraw-Hill.

[6] Todd A. Helwig and Joseph A. Yura, "Torsional Bracing of Columns", Journal of Structural Engineering, Vol.125, No. 5, May, 1999.

[7] Le-Wu Lu, "Derivation of the LRFD Column Design Equations", Engineering Journal / Third Quarter / 2003.

[8] Bjorhovde, Reidar, "Deterministic and probabilistic approaches to the strength of steel columns, Ph.D. dissertation, 1972" (1972). Fritz Laboratory Reports. Paper 1933.

[9] Feng Zhou, Lewei Tong and Yiyi Chen, "Experimental and numerical investigations of high strength steel welded h-section columns" (2013), International Journal of Steel Structures, Vol. 13, No. 2, 209-218.

[10] Wang Yuanqing, Zhu Ruixiang, Dai Guoxin and Shi Gang, "Experimental study on load-carrying behavior of I section steel columns strengthened by welding with initial load" (2014), Journal of Building Structures, Vol. 35, No. 7, 0078-09.